

The Possible Protective Effect of Aldehyde Dehydrogenase 2 Agonist (Alda-1) on Doxorubicin Induced Toxicity of the Left Ventricular Cardiomyocytes of Adult Male Mice

Original
Article

Iman Nabil¹, Wafaa Abdel Rahman Ahmed², Salwa saeed El Sabeh², Rana Ahmed Abouelrous² and Nancy Mohamed El Sekily²

¹Department of Histology and Cell Biology, ²Department of Human Anatomy and Embryology, Faculty of Medicine, Alexandria University, Egypt

ABSTRACT

Background: Doxorubicin (DOX) is an effective antineoplastic drug. However, its cardiotoxicity is a major obstacle that limits its use. Therefore, a novel protective agent is urgently needed. Enzyme activation recently gained much interest as a new therapeutic strategy. In this context, Alda-1 is a newly emerged molecule in the field of cardioprotection through its activation of aldehyde dehydrogenase 2 enzyme.

Aim of the Study: To evaluate the possible protective effect of aldehyde dehydrogenase agonist Alda-1 on doxorubicin induced cardiotoxicity.

Material and methods: Twenty-four adult male C57BL/6 mice were divided equally into 4 groups. Group I received intraperitoneal injection of saline. Group II received intraperitoneal injection of Alda-1 (10 mg/kg) daily for 5 days. Group III received a single intraperitoneal injection of DOX (20 mg/kg). Group IV received both DOX and Alda-1 in the same regimen as in groups II and III, Alda-1 was administered 1 day before DOX. All mice were euthanized on the 5th day following DOX administration. Blood samples were collected, hearts were excised and further processed for anatomical, histological and biochemical analysis.

Results: DOX administration caused extensive cardiotoxicity as evident by the marked decrease in the heart weight and the extensive myocardial lesions shown by the light and electron microscopic examination. Moreover, biochemical serum markers of cardiac injury (CK-MB & LDH) were markedly elevated. Increased oxidative stress was also encountered as shown by the decreased serum TAC and increased tissue MDA. Furthermore, mitochondrial morphometry showed increased mitochondrial size. However, concomitant administration of Alda-1 with DOX has markedly alleviated the heart injury as shown by the restoration of the heart weight and cardiac architecture together with preservation of the mitochondrial structure. Moreover, Alda-1 has ameliorated the biochemical markers of cardiac injury and the oxidative stress.

Conclusion: Alda-1 provides a valuable protective effect against doxorubicin triggered cardiotoxicity.

Received: 24 January 2021, **Accepted:** 10 February 2021

Key Words: Alda-1; aldehyde dehydrogenase 2; cardiotoxicity; doxorubicin; transmission electron microscopy.

Corresponding Author: Rana Ahmed Abouelrous, PhD, Department of Human Anatomy and Embryology, Alexandria Faculty of Medicine, Alexandria, Egypt, **Tel.:** +20 12822 22221, **E-mail:** rana_ahmed86@hotmail.com

ISSN: 1110-0559, Vol. 45, No.1

INTRODUCTION

Doxorubicin (DOX) is regarded as a widely prescribed chemotherapeutic drug. This is owing to its effectiveness against broad spectrum of malignancies^[1]. Unfortunately, this clinical value is combined with special toxic affinity to cardiomyocytes^[2]. Despite the amount of strategies developed to minimize its devastating effect, limited success was observed. And hence, newer drugs are required to restrict its cardiac risks^[3]. DOX-associated damage to cardiac cells is mainly postulated to oxidative injury, Where, DOX imposes oxygen radicals liberation, ultimately endorsing cellular membranes peroxidation with their further degradation and production of toxic aldehydes^[4,5]. Such aldehydes, in turn, are highly reactive, toxic and carcinogenic. They bind to macromolecules intracellularly, like lipids, resulting in their modification,

loss of function and formation of aldehyde adducts with eventual cellular damage^[6].

Aldehyde dehydrogenases are among the enzymatic protective mechanisms against oxidative damage. This is owing to their ability of changing the injurious aldehydes by water soluble organic compounds with reduced toxicity. In such a context, aldehyde dehydrogenase 2 enzyme (ALDH2) can be regarded as the most active of these enzymes with a higher level of expression in the heart tissue^[7,8]. Enzyme activation is viewed as a modern clinical pharmacology tool. It recently gained much interest as it helps in discovering new ways to improve enzymatic performance^[9]. Aldehyde dehydrogenase activator-1 (Alda-1) is a newly emerged molecule that acts as an ALDH2 agonist. It has gained special attention in the field of cardioprotection against various pathologies^[10-13].

DOX can induce a special form of dilated cardiomyopathy. Moreover, DOX was incriminated in inducing inhibition of ALDH2 activity, with particular attribution of oxidative damage and overproduction of injurious aldehydes^[14]. On the other hand, ALDH2 has shown beneficial effect against various types of cardiomyopathies through mitigation of the oxidative stress^[11]. Therefore, the present work was conducted to assess the possible beneficial effect exerted by Alda-1 as an ALDH2 activator against cardiotoxicity triggered by DOX. Yet, according to our best knowledge, publications so far have not investigated this effect on the ultrastructural level of cardiomyocytes using electron microscope. Thus, this study will put much emphasis on the ultrastructural changes induced by DOX and the possible protective effect of Alda-1 on the ventricular cardiomyocytes of adult mice.

MATERIALS AND METHODS

Chemicals

Doxorubicin was obtained as commercial "DOXORUBICIN", EBEWE Pharma production, Austria, as a 50 mg/ 25ml solution. Alda-1 (Tocris Bioscience, UK) was purchased via Clililab Biotechnology Company (Egypt) and was dissolved in normal saline.

Animals

24 adult male C57BL/6 mice from 8-10 weeks old, of average weight 25 g, obtained from the Anatomy and Embryology Animal House Center, Medical faculty, Alexandria. The current study has been approved ethically from Alexandria Medical Faculty Research Committee and was in compliance with the ethical guidelines concerning laboratory animals handling. Mice were granted standard housing and diet conditions.

Experimental design (Figure 1)

The animals were arbitrarily and equally classified in groups of 6.

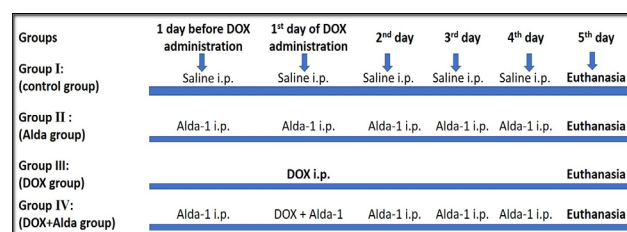


Fig. 1: The Experimental design used.

Group I (control group): mice obtained 0.1 ml saline injection via intraperitoneal (i.p.) route each day for 5 consecutive days^[14,15].

Group II (Alda group): mice obtained 10 mg/kg Alda-1 dissolved in saline i.p. each day for 5 consecutive days^[14,16].

Group III: (DOX group): mice obtained 20 mg/kg body weight of DOX i.p. once^[15].

Group IV (DOX+Alda group): mice received both DOX and Alda-1. DOX was administered as a single i.p. injection in the same dose as in group III. While, Alda-1 administration (10 mg/kg/day i.p. dissolved in saline) started 24 hours prior to DOX administration, for a total duration of 5 consecutive days.

All groups sacrifice was done on the 5th day following DOX administration^[5]. The animals were subjected to anatomical, histological and biochemical studies.

- A. Anatomical examination: On the day of sacrifice, all mice have been weighed and sacrificed by decapitation after ether anesthesia. The hearts were excised and their weights were measured.
- B. Histological examination: The heart apex of all animals, that is mostly formed by the left ventricle, was dissected and processed for light and electron microscopic studies:
 1. Light microscopic study: one part of the tissue was set in 10% formol saline for fixation, then processed by standard procedure to be finally lodged in paraffin. Blocks sectioning was then set at 5 micrometers, and Haematoxylin and Eosin (H&E) was utilized for staining^[17].
 2. Ultrastructural study: the second parts of the specimens were immediately cut into smaller pieces (~1 mm³), preserved in 3% phosphate-buffered gluteraldehyde solution with further processing for transmission electron microscopic (TEM) examination. The grids examination and photographing were performed using JEOL JEM-1400 Plus (Tokyo, Japan) TEM, Faculty of Science, University of Alexandria^[18].
- C. Biochemical study of cardiac enzymes and oxidative stress markers: blood samples have been drawn from the abdominal aorta of all mice for biochemical analysis. They were centrifuged and blood sera were collected for measurement of cardiac enzymes and Total Antioxidant defence. Remaining cardiac tissue portion was processed for the analysis of the toxic aldehyde malondialdehyde (MDA) to guide for oxidative stress.

Measurement of cardiac enzymes: assessment of Creatine kinase- MB (CK-MB) together with lactate dehydrogenase (LDH) within mice sera as biomarkers of cardiac tissue injury was done. They were estimated by using Spectrum diagnostic kit (Hannover, Germany) in U/L by following the manufacturer's procedures.

Measurement of total antioxidant capacity: as a marker of antioxidant defense state, was done using Biodiagnostic kit (Giza, Egypt) by following the kit procedure and results were expressed as mM/L.

Measurement of oxidative stress: Malondialdehyde (MDA) concentration was assessed using supernatant of the homogenized heart tissue as a marker of lipid peroxidation and oxidative stress. It was determined using diagnostic kit of Biodiagnostic (Giza, Egypt) in nmol/g. tissue by following the manufacturer's instructions.

D. Morphometric study: Mitochondrial size: Electron photomicrographs were used to assess the mitochondrial size. Photomicrographs with numerous mitochondria with microscopic magnification of $\times 5000$ were used. After converging pixels to micrometers, manual tracing of the mitochondrial boundaries was done to assess mitochondrial size by Image J software (version 1.53f). In order to ensure accurate evaluation of mitochondrial size, exclusion of the mitochondria on the periphery of the images was done^[19].

Statistical analysis

The biochemical results and the morphometric measurement were statistically analyzed by SPSS software (version 20.0). Normal distribution verification was settled using Kolmogorov-Smirnov test. Quantitative data have been presented by range, mean, standard deviation and median^[20].

RESULTS

A. Anatomical results

Mice body weight in DOX group (group III) was shown to be significantly decreased in comparison to that of the control group (group I) as well as the Alda group (group II). Concerning the DOX+Alda group (group IV), although the body weight in this group was higher as regarding that of DOX group, this increase was not statistically significant. (Figure 2)

Regarding the heart weight, following administration of DOX, the mean heart weight in group III was significantly decreased in contrast to all other groups. In contrary, the mean heart weight in group IV (DOX+Alda group) revealed no significant difference in comparison with the control and Alda groups, whereas it was significantly increased as compared to group III (Figure 3).

B. Histological results

1. Light microscopic examination of left ventricular myocardium using Hematoxylin & Eosin stain:

Control group (group I)

Myocardial sections revealed normal cardiac tissue features. Cardiac fibers were seen branching and running in different directions with narrow interstitial spaces. They exhibited acidophilic sarcoplasm and oval vesicular centrally located nuclei. Nuclei of connective tissue cells were also encountered within the endomysium between the muscle fibers (Figure 4).

Alda group (group II)

Examination of myocardial sections of Alda group showed normal histological pattern of cardiomyocytes possessing acidophilic sarcoplasm with central vesicular nuclei (Figure 5).

DOX group (group III)

Histological examination of DOX treated group revealed evident myocardial alterations in the form of distorted cardiac muscle fibers with wide interstitial spaces along with focal interruption of continuity up to complete loss of muscle fibers (Figure 6). Waviness of many fibers (Figure 7) together with wide areas of degeneration were noticed as well (Figures 8,9). Focal areas of deeply stained homogeneous sarcoplasm devoid of striations typical of hyalinosis were frequently encountered (Figure 9). Some fibers showed pale acidophilic sarcoplasm (Figures 6b,8b), while others showed patchy hyperoesinophilia (Fig. 6b). Darkly stained nuclei (Figures 7,8) were also encountered. In addition, many muscle fibers appeared with vacuolated sarcoplasm (Figures 9,10,11), these findings were sometimes accompanied with foci of cellular infiltration and extravasated red blood corpuscles (RBCs) (Figures 10-12).

Alda+DOX group (group IV)

Examinations of myocardial sections of this group showed almost preservation of normal pattern of the cardiac myofibers with acidophilic sarcoplasm and vesicular nuclei together. Some areas show narrow interstitial spaces but others were still wide. Nevertheless, persistence of some foci of pale acidophilic sarcoplasm within the myofibers were still encountered (Figure 13).

2. Electron microscopic examination:

Control group (group I)

Electron microscopic examination of left ventricular myocardium of control group, revealed cardiomyocytes with well-organized myofibrils separated by rows of elongated mitochondria with tightly packed cristae. The myofibrils showed normal striation pattern, where the dark A band is bisected by light H zone. The latter is further bisected by a dense M line. The light I band is bisected by a dense Z line, thus the sarcomere could be observed extending between two successive Z lines. T-tubules were noticed at the level of the Z line. Each cardiomyocyte exhibited an elongated centrally located nucleus with prominent nucleoli. Aggregates of mitochondria at the nuclear poles were further revealed. Adjacent cardiomyocytes were connected by step wise intercalated discs with intact transverse and longitudinal components. (Figure 14).

Alda group (group II)

Examination of the left ventricular cardiac muscle fibers of Alda group showed almost normal characteristics of the cardiomyocytes with regular myofibrils arrangement

and sarcomere banding along with elongated centrally located nuclei. Cardiomyocytes were joined end to end by intact intercalated discs (Figure 15).

DOX group (group III)

Examination of the left ventricular myocardium of DOX group, revealed evident cardiomyocytic changes. The sarcolemma showed scalloping and localized blebbing (Figure 16). Cardiac myofibrils appeared disorganized with abrupt thinning, interruption, and loss of alignment as well as areas of complete myofibril loss. Areas of disintegration and vacuolation of the myofibrils were detected as well (Figures 16-19). Many cardiomyocytes exhibited focal myofibrillar hypercontraction with closely approximated Z-lines and contracted sarcomeres (Figure 20). Mitochondrial alterations were further revealed in the form of irregularly arranged mitochondria with dense matrix, vacuolated, bizarre-shaped and with disrupted cristae (Figures 16,18,19). Lysosomes and autophagosomes could be seen in the sarcoplasm as well (Figures 16,18). Other detectable lesions included dilated profiles of sarcoplasmic reticulum (Figure 17) and irregular nuclei with peripheral condensation of its chromatin (Figure 18). As for the intercalated discs, they occasionally revealed wide separation of the transverse portions with focal areas of disruption (Figure 19). In addition, noticeable foci of collagen fiber deposition in the interstitial spaces were seen (Figure 21).

Alda+DOX group (group IV)

Ultrastructural examination of the left ventricular myocardium of group IV showed evident preservation of the cardiomyocytes. Most of them exhibited apparently normal appearance with well-organized myofibrils. The sarcolemma was almost straight. The sarcomeres showed normal striation pattern with characteristic light and dark

bands. Only few cardiomyocytes showed focal areas of disintegrated myofibrils. Apparently normal nuclei were seen in the cardiomyocytes with central location and normal chromatin distribution. The intercalated discs appeared intact (Figure 22).

C. The biochemical results

Measurement of cardiac enzymes: In the present work, the serum values of CK-MP & LDH following administration of DOX in group III revealed significant increase in contrast to control and Alda groups. While in group IV, which received both DOX and Alda-1, both enzymes showed significant decrease as compared to group III and non-significant difference in relation to control and Alda groups (Figures 23,24).

Measurement of the total antioxidant capacity and the oxidative stress markers: The antioxidant defense as demonstrated by the serum levels of total antioxidant capacity revealed significant decline in DOX group in contrast to all other studied groups, while in DOX+Alda group, it was significantly increased contrasted to DOX group. Additionally, the mean value of tissue MDA showed significant increase within DOX group in contrast with control and Alda groups. While following Alda-1 administration in group IV, a non-significant decrease of MDA level was revealed in comparison to the other three groups (Figures 25,26).

D. Morphometric results

Mitochondrial size: Morphometric analysis of mitochondrial size showed significant increase in group III than all other comparative groups, indicating swelling of the mitochondria. While Alda + DOX group demonstrated no significant difference as opposed to control and Alda groups (Figure 27).

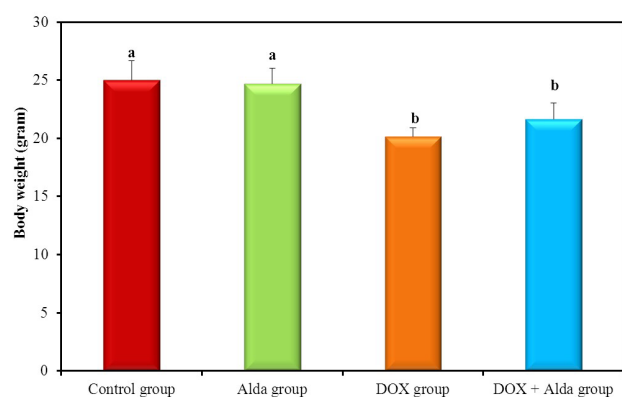


Fig. 2: A bar chart comparing experimental groups body weight (in gram). Identical letters show insignificance, whereas means having dissimilar letters show significance. Statistical significance at $p \leq 0.05$. $n=6$

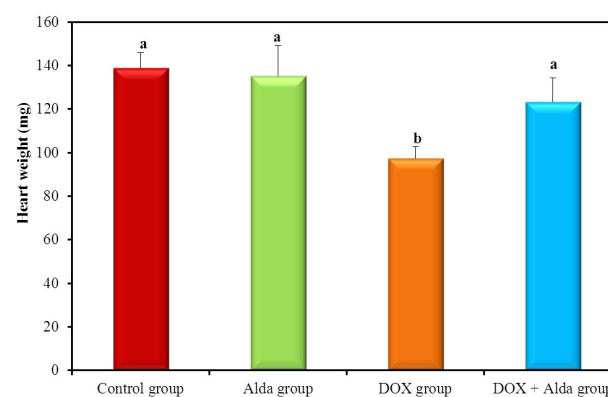


Fig. 3: A bar chart comparing experimental groups heart weight (in mg). Identical letters show insignificance, whereas means having dissimilar letters show significance. Statistical significance at $p \leq 0.05$. $n=6$

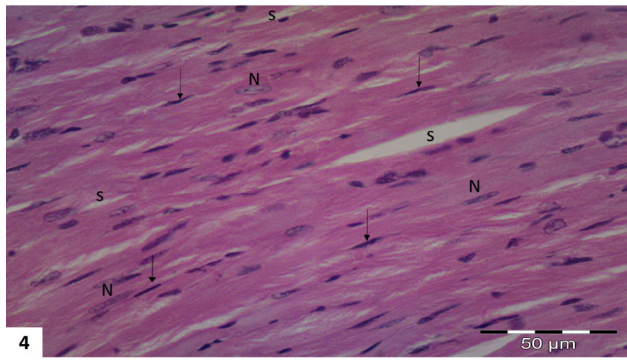


Fig. 4: A photomicrograph of left ventricular myocardium of group I (control group) revealing acidophilic branching and anastomosing cardiac muscle fibers with centrally located vesicular nuclei (N). Notice flattened nuclei of fibroblasts (arrows) and the narrow interstitial spaces (S). (Haematoxylin and Eosin stain, microscope magnification $\times 400$)

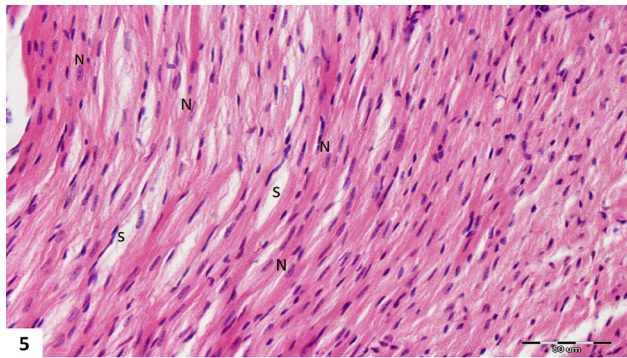


Fig. 5: A photomicrograph of left ventricular myocardium of group II (Alda group) demonstrating almost normal looking cardiac muscle fibers. Notice vesicular cardiomyocytes nuclei (N) and narrow interstitial spaces (S). (Haematoxylin and Eosin stain, microscope magnification $\times 400$)

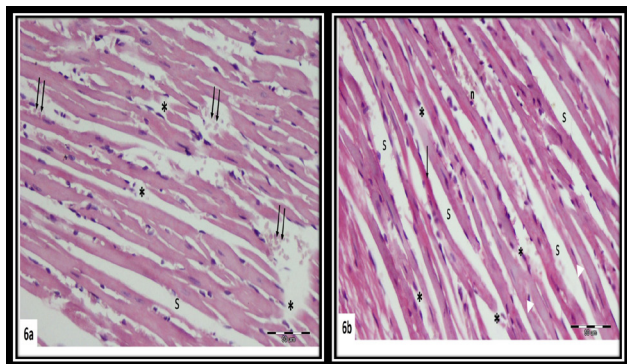


Fig. 6: Photomicrographs of doxorubicin treated left ventricular myocardium (group III) showing localized areas of interrupted muscle fibers and complete fiber loss (*). Some fibers show pale acidophilic sarcoplasm (white arrow heads), others exhibit localized hyper eosinophilia (arrow). Fig. (a) showing extravasated RBCs (Double arrows), while Fig. (b) showing small darkly stained nucleus (n). Notice, the wide interstitial space (S). (Haematoxylin and Eosin stain, microscope magnification $\times 400$)

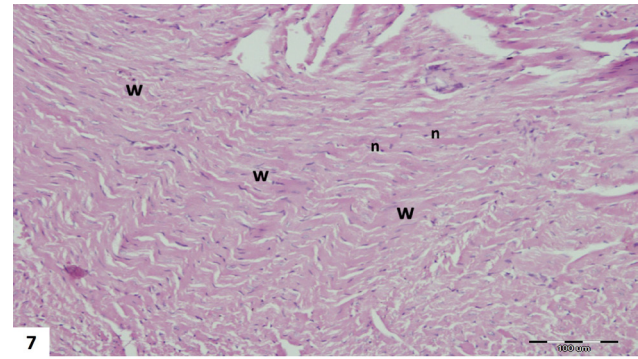


Fig. 7: A photomicrograph of group III ventricular myocardium showing evident wavy (w) muscle fibers with deeply stained nuclei (n). (Haematoxylin and Eosin stain, microscope magnification $\times 400$)

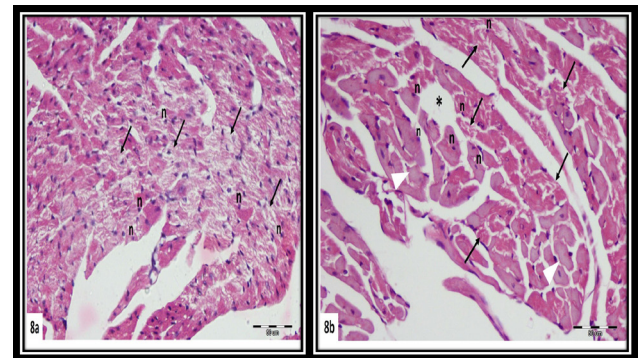


Fig. 8: Photomicrographs of left ventricular myocardium of DOX group (group III), revealing distorted muscle fibers with wide areas of degeneration (arrows) as well as small, dark nuclei (n). Notice pale acidophilic sarcoplasm of some myofibers (white arrow heads) and focal loss of others (*) in Fig. (b). (Haematoxylin and Eosin stain, microscope magnification $\times 400$)

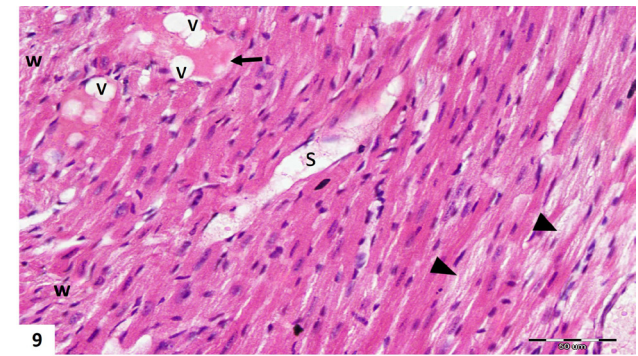


Fig. 9: A photomicrograph of left ventricular myocardium of group III depicting areas of homogeneous acidophilic and vacuolated (V) muscle fibers devoid of striations (arrow). Focal areas of degeneration (arrow heads) are also seen together with evident wavy (w) muscle fibers. Notice, the wide interstitial space (S). (Haematoxylin and Eosin stain, microscope magnification $\times 400$)

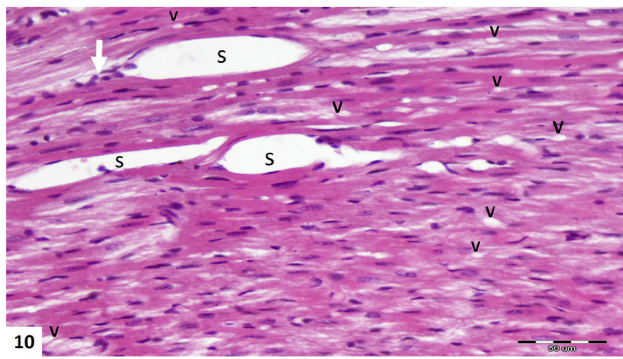


Fig. 10: A photomicrograph of group III myocardium showing some muscle fibers with sarcoplasmic vacuoles (V). Focal cellular infiltration (white arrow) can also be encountered. Notice, wide interstitial spaces (S). (Haematoxylin and Eosin stain, microscope magnification $\times 400$)

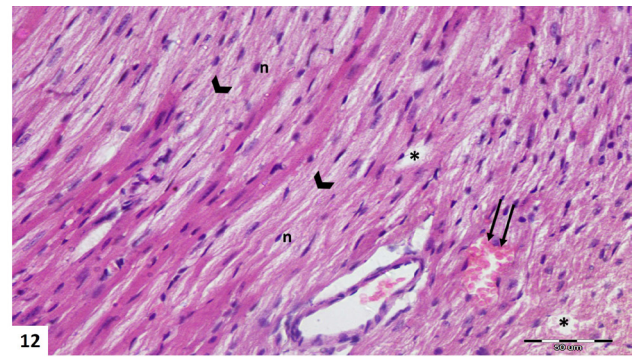


Fig. 12: A photomicrograph of the left ventricular myocardium of group III depicting wide areas of degeneration with pale acidophilic sarcoplasm (<) and deeply stained nuclei (n). Congested blood capillary (double arrow) can also be encountered. Notice focal loss of some muscle fibers (*). (Haematoxylin and Eosin stain, microscope magnification $\times 400$)

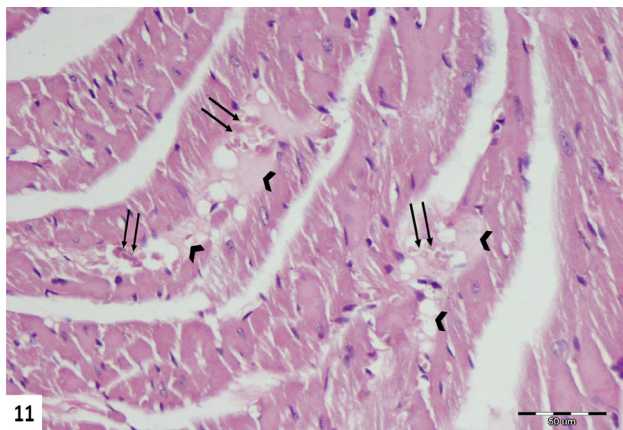


Fig. 11: A photomicrograph of left ventricular myocardium of group III revealing pale vacuolated appearance of some muscle fibers (<) and extravasated RBCs (double arrows). (Haematoxylin and Eosin stain, microscope magnification $\times 400$)

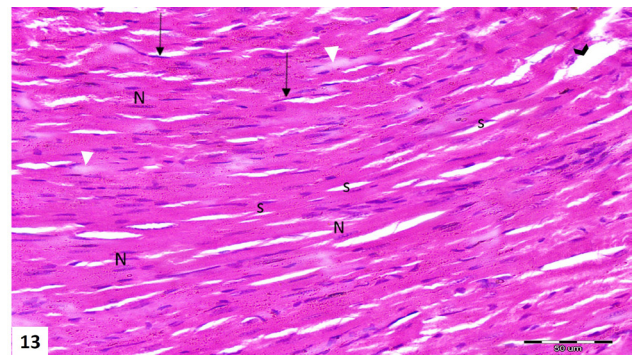


Fig. 13: A photomicrograph of group IV myocardium (received doxorubicin and alda-1) showing apparently normal cardiac muscle fibers with centrally located, vesicular nuclei (N). Some muscle fibers still depict foci of pale sarcoplasm (white arrowhead). Flattened nucleus of fibroblast are also seen (arrows). Some areas show narrow interstitial spaces (S) but others are still wide (arrow head) (Haematoxylin and Eosin stain, microscope magnification $\times 400$)

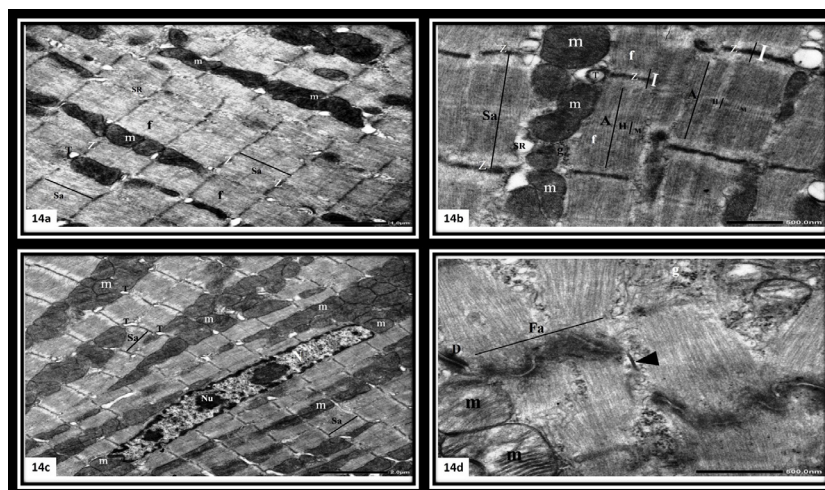


Fig. 14: TEM photomicrographs of control ventricular myocardium (group I) revealing: (a): a cardiomyocyte with well-organized myofibrils (f). The mitochondria (m) are arranged in rows between the myofibrils. Sarcomeres (Sa) are well ordered. T- tubules (T) are seen at the level of Z line (Z). Sarcoplasmic reticulum tubules (SR) can also be noticed. (b): a high magnification of the myofibrils showing the characteristic banding pattern of the sarcomeres (Sa): the dark band (A) is bisected by a lighter zone (H) which is further bisected by a narrow dense M-line (M), The light band (I) is bisected by a dense Z line (Z). Glycogen granules (g) are also seen. (c): a cardiomyocyte exhibits an elongated central nucleus (N) with prominent nucleoli (Nu). Multiple mitochondria (m) are seen at the nuclear poles and in between the myofibrils. (d): The intercalated disc showing a stepladder course with a transverse part composed of fascia adherens (Fa) and desmosomes (D) and a longitudinal part having gap junctions (arrow head). (Microscope magnification a $\times 5000$, b $\times 10,000$, c $\times 3000$, d $\times 15,000$)

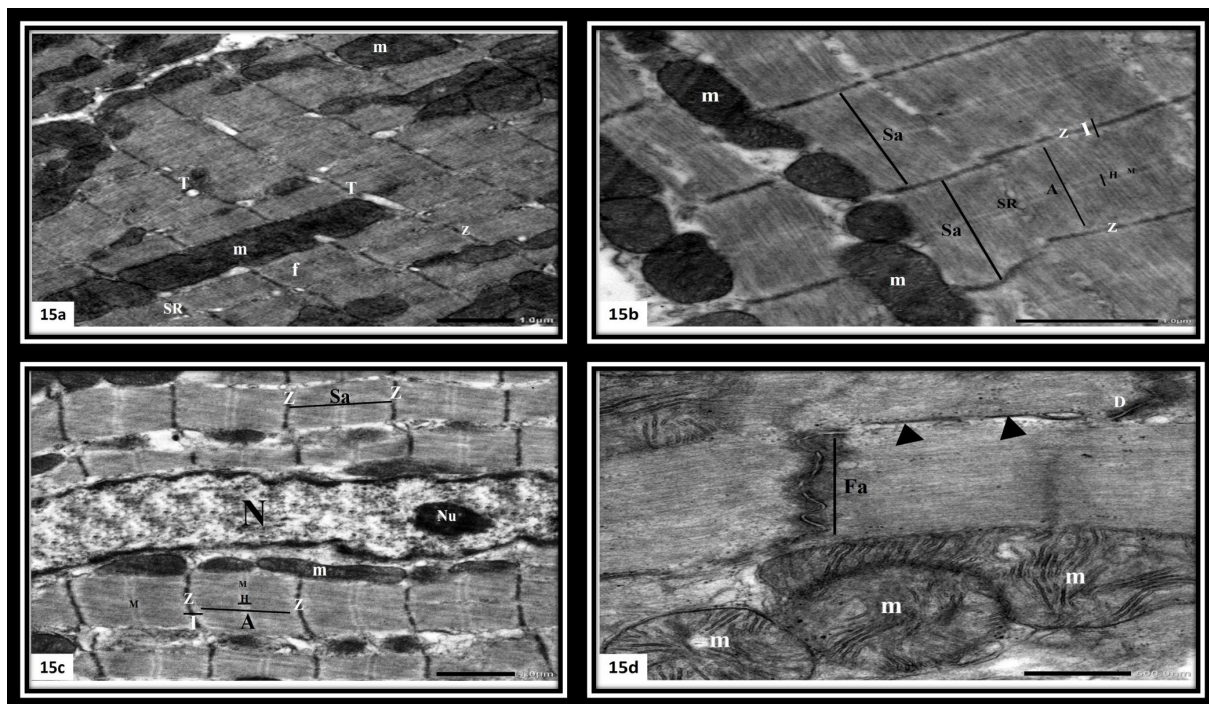


Fig. 15: TEM photomicrographs of ventricular myocardium of group II (Alda group) revealing: (a): well organized myofibrils (f) with normal cross banding pattern. The mitochondria (m) are arranged in rows between the myofibrils. The sarcoplasmic reticulum tubules (SR) are spanning the sarcomere together with encountered transverse tubules (T) at the level of the Z line (Z). (b): well registered sarcomeres (Sa) with its characteristic banding pattern: the dark band (A) is bisected by a lighter zone (H) which is further bisected by a narrow dense M-line (M). The light band (I) is bisected by a dense Z line (Z). (c): a cardiomyocyte exhibits an elongated, centrally located nucleus (N) with prominent nucleolus (Nu). (d): an intact intercalated disc with its transverse part appears as a dense folded line composed of desmosome (D) and fascia adherens (Fa) and longitudinal component composed of gap junction (arrow head). (Microscope magnification a & c $\times 5000$, b $\times 8000$, d $\times 12,000$)

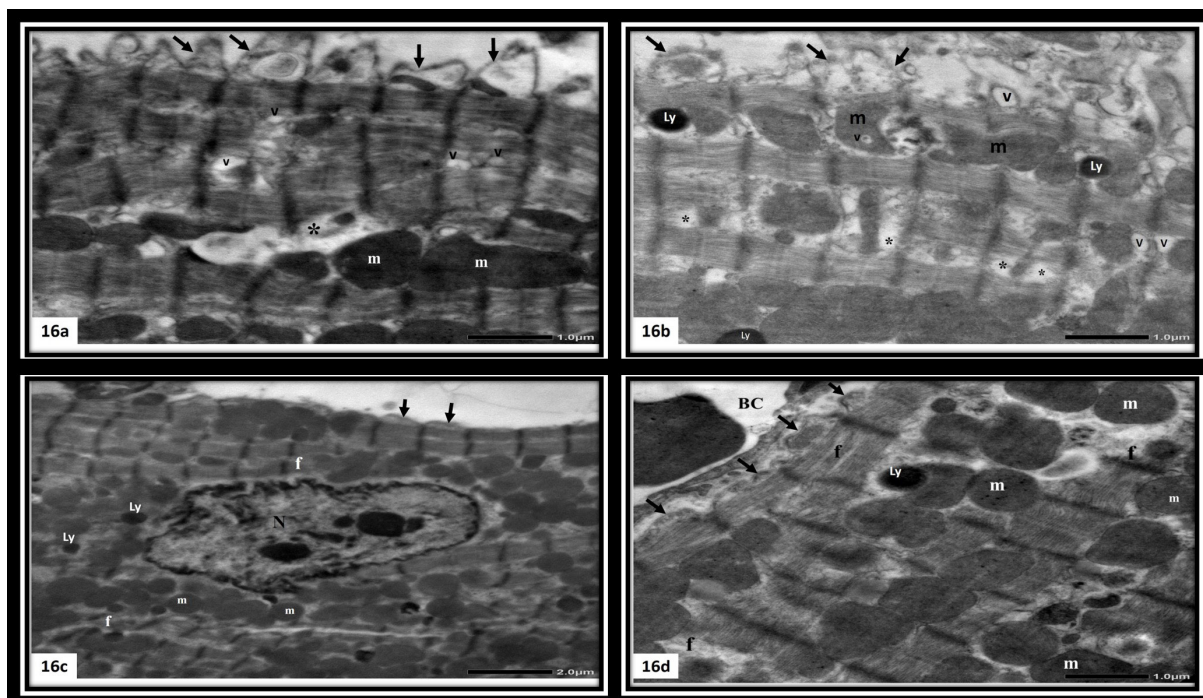


Fig. 16: TEM photomicrographs of doxorubicin treated myocardium (group III) showing: (a&b) the cardiomyocytes depict thin interrupted myofibrils (*) with scalloping and localized blebbing of the overlying sarcolemma (↑). Multiple vacuoles (V) are also seen. In Fig. a, the mitochondria (m) appear with dense matrix, while in Fig. b, bizarre-shaped and vacuolated mitochondria (m) are seen. (c&d) disordered myofibrils (f) with irregularly arranged mitochondria. Numerous lysosomes are also seen (Ly). Notice, the irregular cardiomyocyte nucleus (N) in Fig. (c) and blood capillary in the endomysium (BC) in Fig. (d). (Microscope magnification a,b&d $\times 5000$, c $\times 2500$)

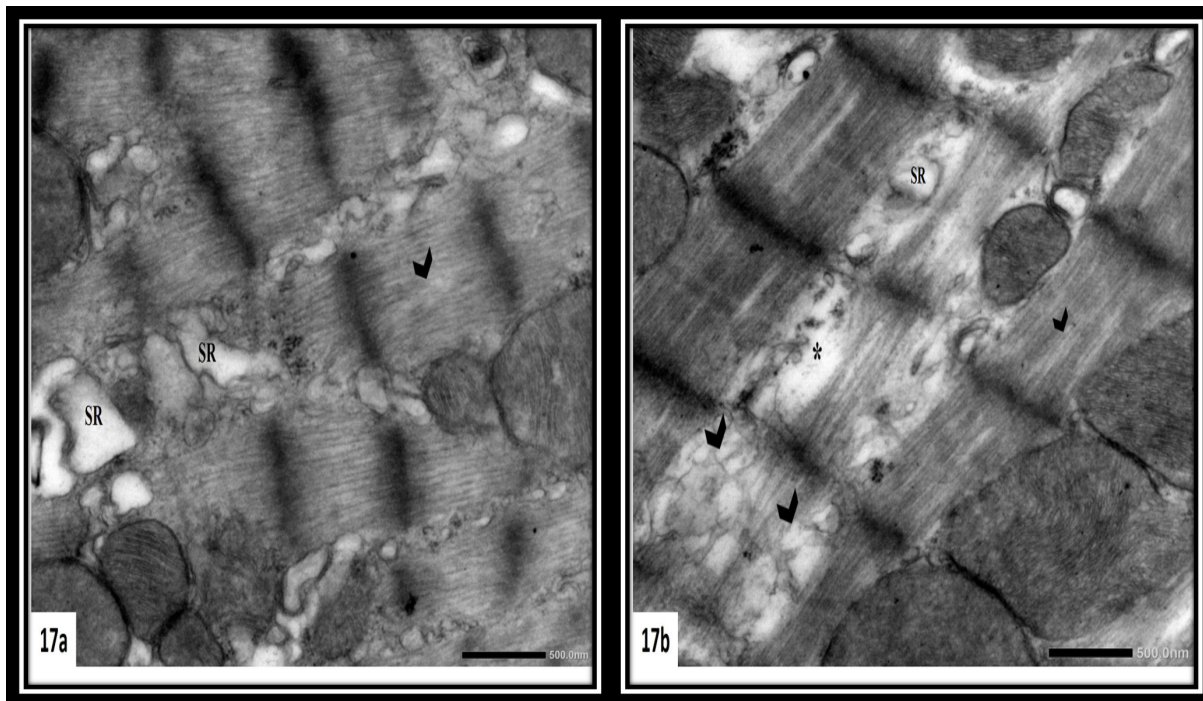


Fig. 17: TEM photomicrographs of left ventricular cardiomyocytes of group III revealing disrupted myofibrils (<) with areas of focal loss and disintegration (*). Dilated profiles of sarcoplasmic reticulum (SR) are also seen. (Microscope magnification a&b×10,000)

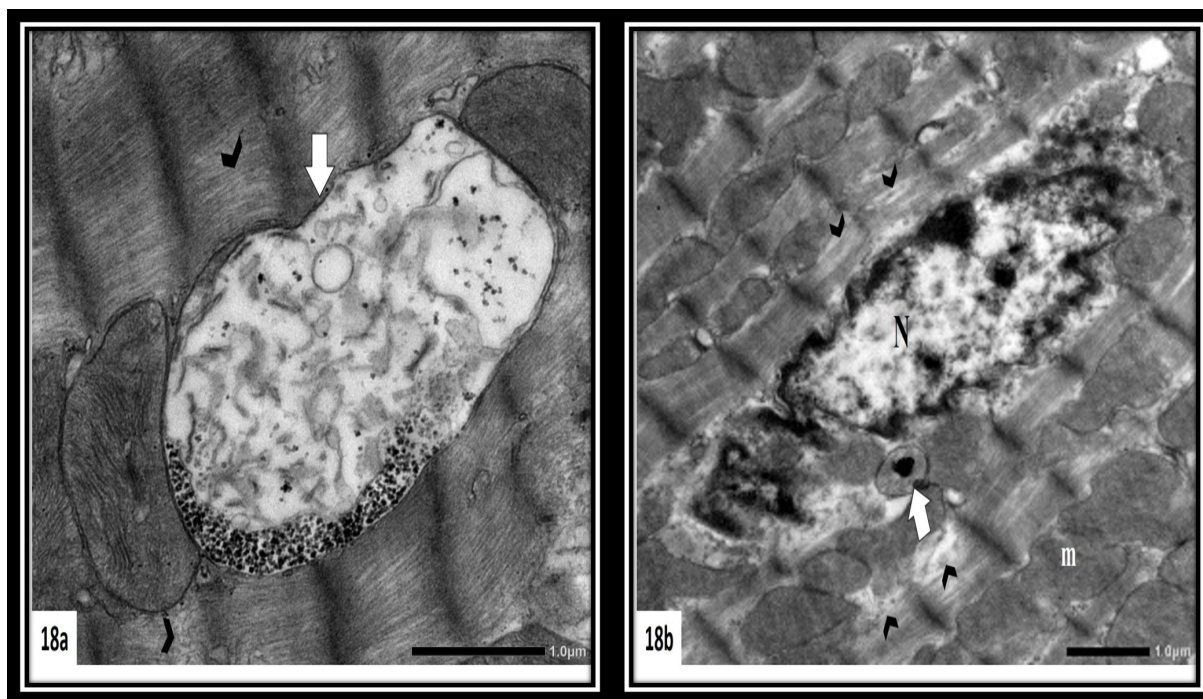


Fig. 18: TEM photomicrographs of ventricular myocardium of group III showing membrane-bounded structures with degenerated contents (arrow) indicative of autophagic vacuoles. Focal areas of fibrillar disintegration (<) are noticed. Irregular cardiomyocyte nucleus (N) together with bizarre-shaped mitochondria (m) are also observed in Fig. (b). (Microscope magnification a ×8,000, b×5000)

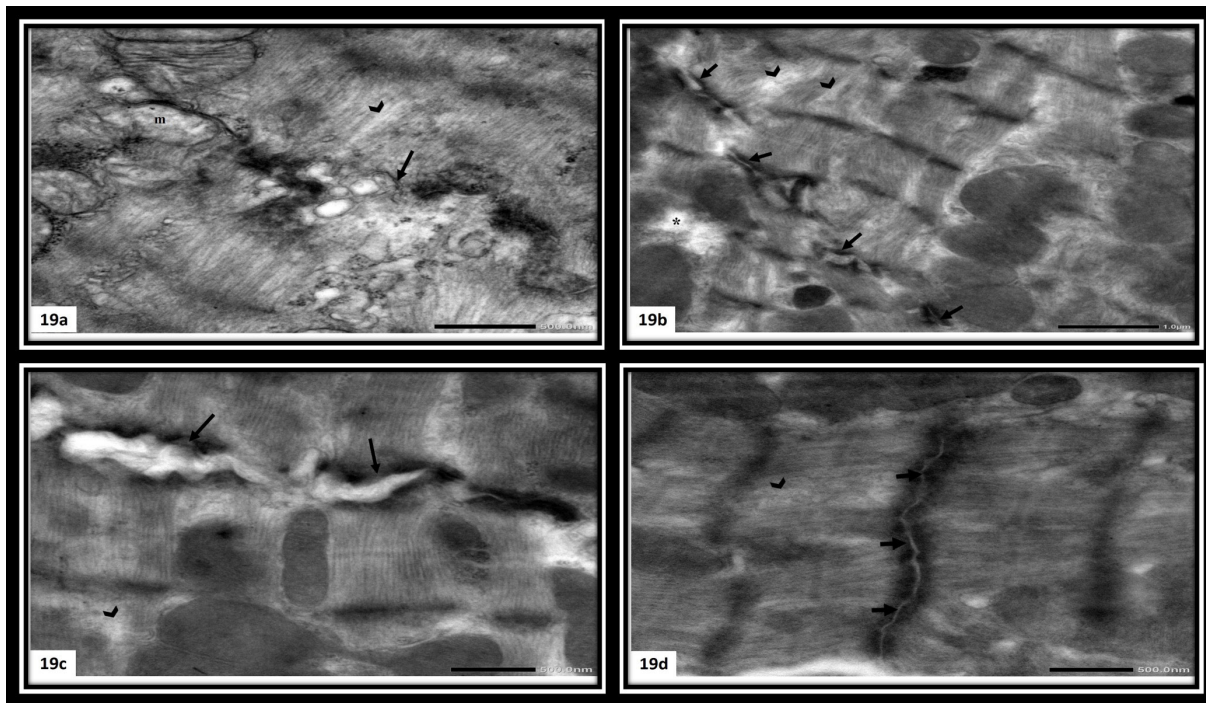


Fig. 19: TEM photomicrographs of ventricular myocardium of group III showing disrupted intercalated discs (arrow) with widely separated transverse portions (at b&c) and abnormal straightening (at d). Focal areas of myofibrillar loss (*) and disintegration (<) are also seen. Notice some mitochondria (m) with disrupted cristae in Fig. a. (Microscope magnification a $\times 12,000$, b $\times 6000$, c&d $\times 10,000$)

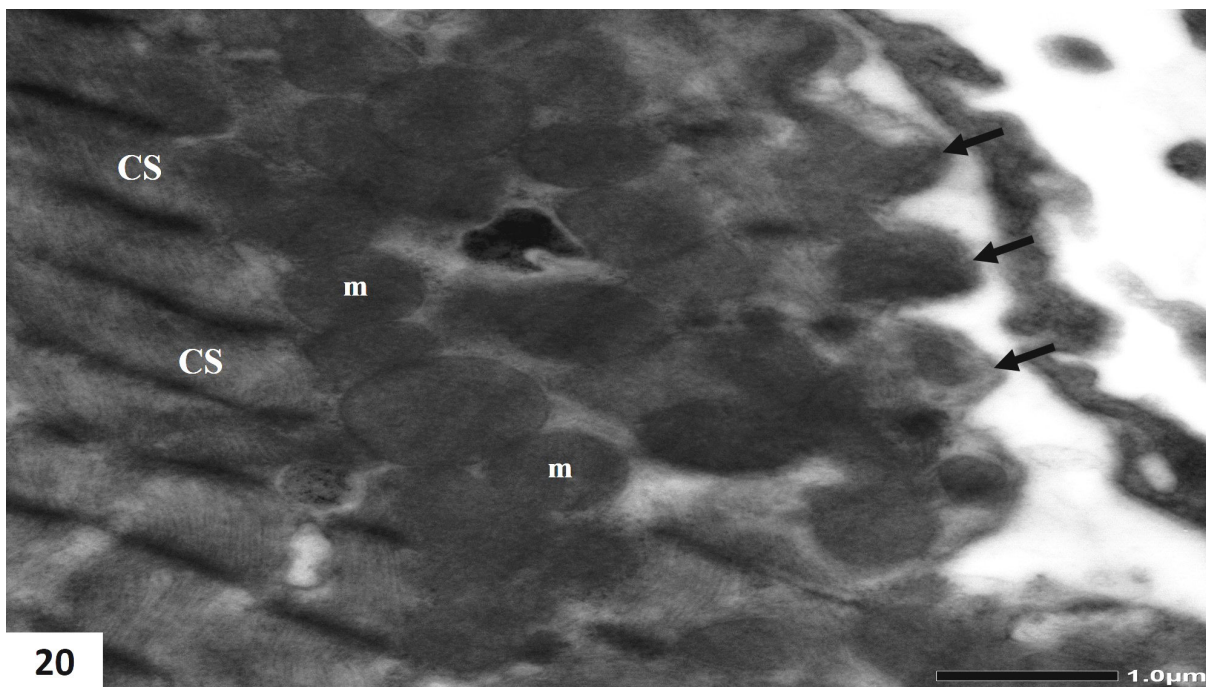


Fig. 20: A TEM photomicrograph of left ventricular myocardium of group III showing the formation of contracted sarcomeres (CS) with scalloping of the overlying sarcolemma (↑). Irregularly arranged mitochondria (m) are also seen. (Microscope magnification $\times 5000$)

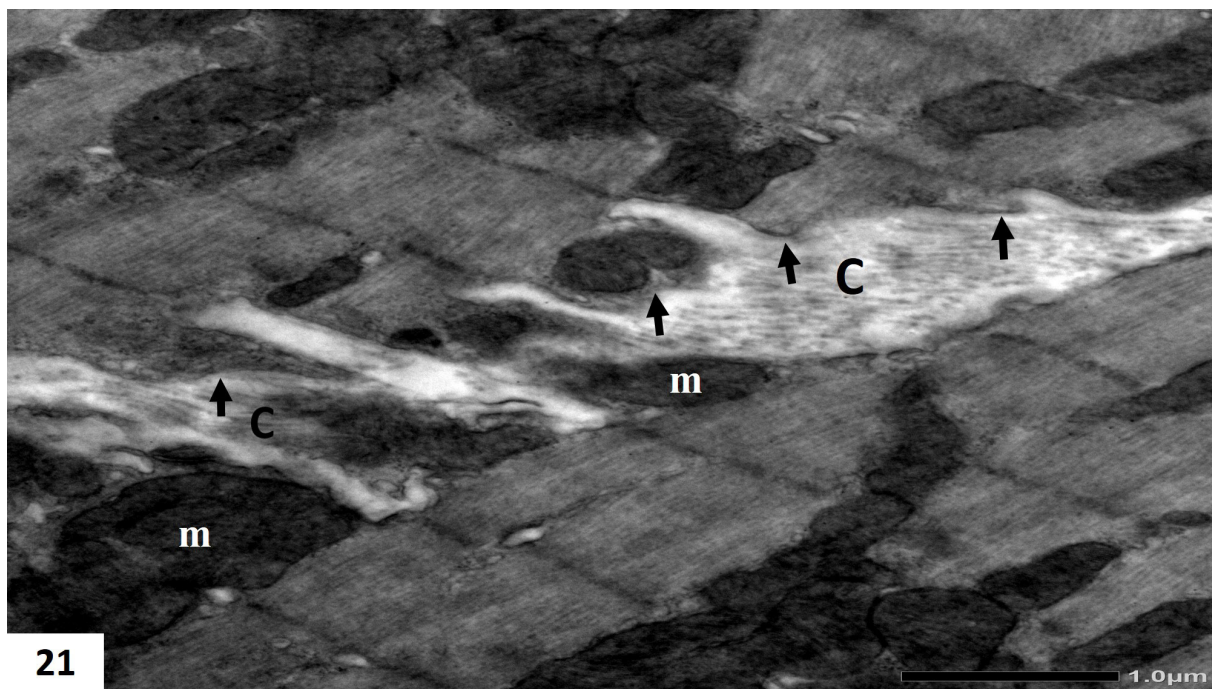


Fig. 21: A TEM photomicrograph of ventricular myocardium of group III revealing some collagen fibers (C) occupying the interstitial space between two adjacent cardiomyocytes. Notice the scalloped sarcolemma (↑). Mitochondria (m) can be also seen under the sarcolemma. (Microscope magnification ×6000)

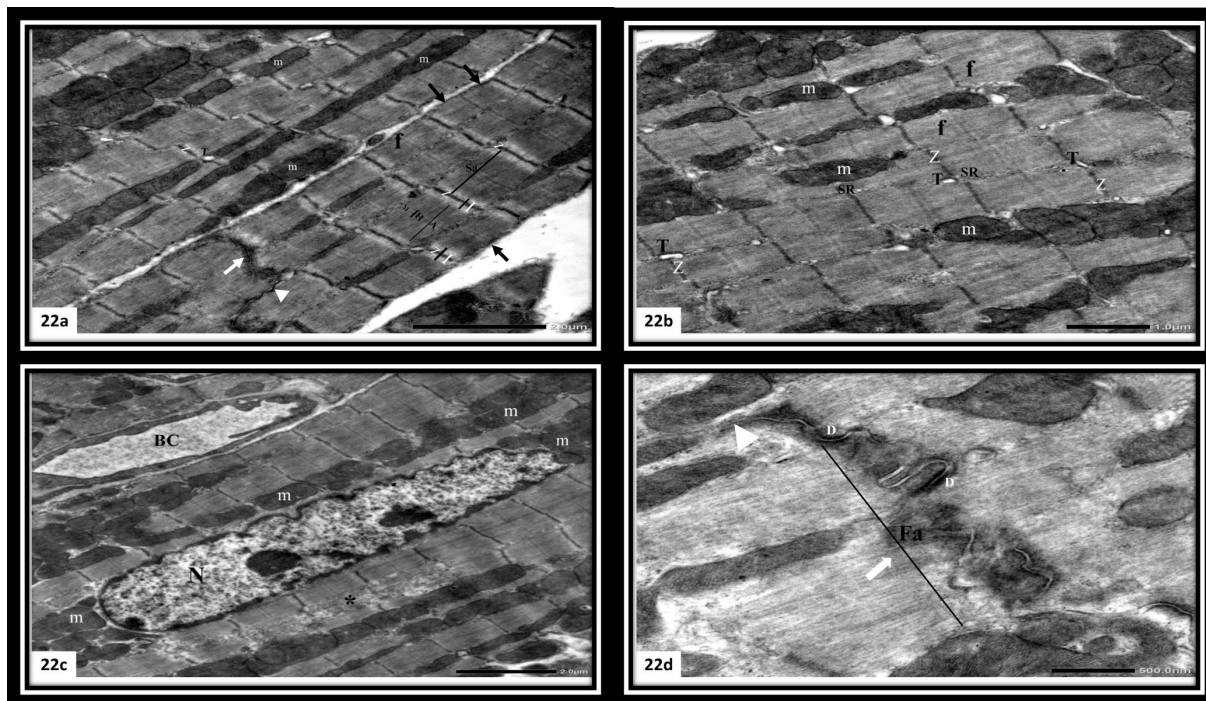


Fig. 22: TEM photomicrographs of the left ventricular myocardium of group IV (DOX+Alda group) revealing: (a&b) regularly arranged myofibrils (f) with normal cross banding appearance. The sarcolemma appears almost straight (↑). Elongated mitochondria (m) are arranged in rows between the myofibrils. Sarcomeres (Sa) are well ordered showing the characteristic banding pattern where the dark band (A) is bisected by a lighter zone (H) which is further bisected by a narrow dense M line (M). The light band (I) is bisected by a dense Z line (Z). Sarcoplasmic reticulum tubules (SR) and T-tubule (T) are also seen. (c): A cardiomyocyte shows interrupted myofibrils with loss of identifiable sarcomeres (*). Notice, the elongated centrally located euchromatic nucleus (N) and the blood capillary (BC) in the endomygium. (d): an intact intercalated disc with normal transverse (white arrow) and longitudinal (arrowhead) components. The Transverse component is formed of desmosome (D) and fascia adherens (Fa). (Microscope magnification a×4000, b×5000, c×3000, d×10,000)

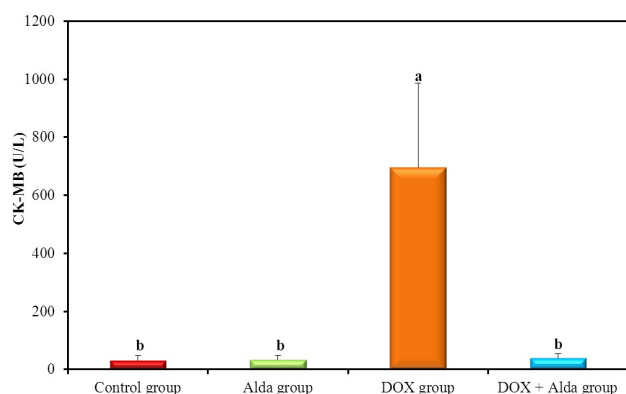


Fig. 23: A bar chart comparing experimental groups CK-MB (in U/L). Identical letters show insignificance, whereas means having dissimilar letters show significance. Statistical significance at $p \leq 0.05$. n=5

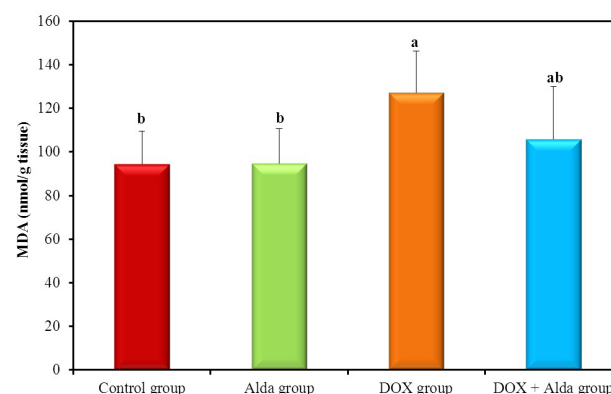


Fig. 26: A bar chart comparing experimental groups MDA (nmol/g tissue). Identical letters show insignificance, whereas means having dissimilar letters show significance. Statistical significance at $p \leq 0.05$. n=5

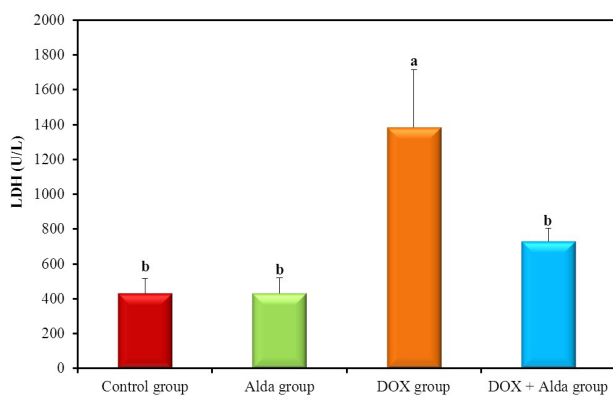


Fig. 24: A bar chart comparing experimental groups LDH (in U/L). Identical letters show insignificance, whereas means having dissimilar letters show significance. Statistical significance at $p \leq 0.05$. n=5

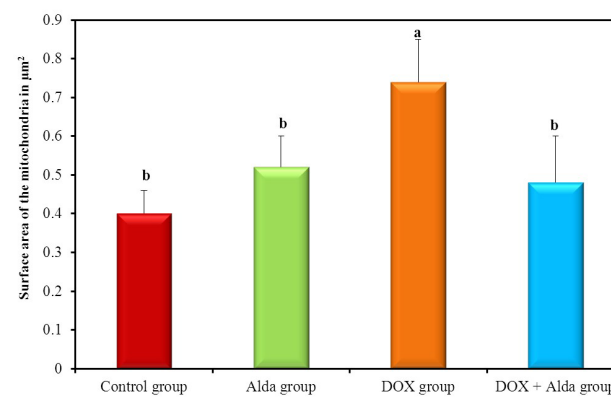


Fig. 27: A bar chart comparing experimental groups mitochondrial size (in µm²). Identical letters show insignificance, whereas means having dissimilar letters show significance. Statistical significance at $p \leq 0.05$. n=5

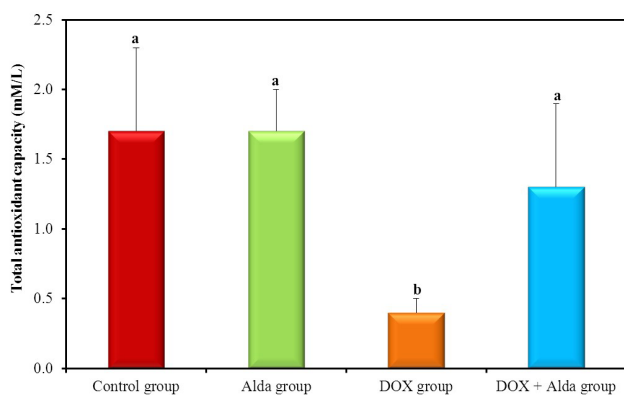


Fig. 25: A bar chart comparing experimental groups total antioxidant capacity (in mM/L). Identical letters show insignificance, whereas means having dissimilar letters show significance. Statistical significance at $p \leq 0.05$. n=5

DISCUSSION

Doxorubicin is a highly utilized antineoplastic drug, although it is capable of causing significant heart toxicity and irreversible cardiomyopathy in medical practice^[21]. Despite the fact that, several compounds were tested in attempt to lessen the cardiac injury attributed to DOX, they showed limited beneficial value^[22-24]. In line with the previously mentioned facts, it seems quite essential to evaluate the protective effect of a novel cardioprotective agents on DOX-triggered cardiotoxicity. Therefore, the current work was designed to illustrate probable defensive effect of Alda-1 on DOX-triggered cardiotoxicity.

Alda-1, is a newly recognized ALDH2 agonist, that is capable of activating ALDH2 catalytic activity and subsequently improves its interaction with different

substrates. Moreover, it acts as a molecular chaperon (molecule that promotes proper folding and assembly of other macromolecules); thus enhancing ALDH2 folding in a proper manner. Interestingly, it is even capable of amending the structural defects of the enzyme mutant form (ALDH2*2), the most prevailing human single point mutation^[25,26]. Several studies unveiled that Alda-1 through being ALDH2 agonist was able to protect against different pathologies through alleviation of oxidative stress and injurious aldehydes like 4-hydroxy-2-nonenal (4HNE) as well as malondialdehyde (MDA) together with preservation of mitochondrial function^[12,27-29]. The current work demonstrated that Alda-1 administration was capable to a large extent to guard against DOX-induced cardiomyopathy.

The present study has been performed on the widely used C57BL/6 mouse strain as it represents the best model of DOX cardiotoxicity^[30,31]. Thus its use enhances the reproducibility and further extension of investigations in other researches^[32]. Doxorubicin dose regimen adopted in the current work was in compliance with reports in previous studies for induction of acute DOX cardiomyopathy in adult male mice^[5,15,33].

In the current work, administration of Alda-1 alone in group II mice displayed no differences in relation to the control group regarding all the studied parameters. On the other hand, DOX group has shown significant decrease in both body weight and heart weight. Willis *et al.*^[32] have detected decline in heart mass in humans by cardiac MRI as early as one month after DOX exposure. They also demonstrated similar decline in heart weight in experimental mice exposed to DOX. This reduction in the heart weight might be attributed to either atrophy^[32], or actual death of the muscle fibers induced by DOX intoxication^[34,35]. Our data demonstrated that Alda-1 ameliorated DOX-triggered reduction in the heart weight, where Alda+DOX group manifested significant escalation in the heart weight as compared to group III mice. However, Alda-1 couldn't rescue the decreased body weight induced by DOX, which might be attributed to accompanying factors such as loss of appetite and dehydration^[33,36].

Histological examination using light and electron microscopes in DOX treated group went in accordance with previous studies^[37-40] as it has revealed extensive myocardial lesions in the form of myofiber degeneration, disintegration and focal loss together with degenerative changes of the sarcoplasmic organelles and even the sarcolemma. Moreover, biochemical markers of cardiac tissue injury CK-MB and LDH were significantly raised in mice sera after DOX exposure. These cardiac enzymes escape from the intracellular compartment of the damaged cardiomyocytes into the blood. Therefore, their blood levels are correlated to the degree of cardiac tissue damage^[41,42]. In addition, total antioxidant capacity (TAC) in mice sera showed significant decrease in DOX group than the other studied groups. Such decrease in the TAC is a sign of oxidative stress and indicates the vulnerability

to oxidative damage^[43,44]. Moreover, lipid peroxidation was raised significantly as shown by the raised tissue MDA levels in DOX group which went in accordance with the previous literature^[5,15,45,46].

The predominant mechanism by which DOX damages the cardiomyocytes is oxidative stress dependent. This leads to subsequent lipid peroxidation and toxic aldehydes liberation^[47,48]. Moreover, the cardiac muscles are known to possess reduced level of antioxidant enzymes, thus restricting their detoxification ability. In addition, DOX is capable of inhibiting antioxidant enzyme activity, therefore increasing the cardiomyocyte vulnerability to oxidative stress^[47].

Mitochondria are the main target organelle affected by doxorubicin^[49]. It is concentrated inside the mitochondria due to its attraction to a mitochondrial phospholipid named cardiolipin^[48,50]. Mitochondrial damage could be attributed to DOX-triggered lipid peroxidation of cellular membranes, which leads to damage of their integrity and alteration of their fluidity, this eventually causes dysfunction and inactivation of the proteins bounded by these membranes^[51]. In addition, reactive aldehydes can escalate mitochondrial mediated development of reactive oxygen species (ROS) and alter its membrane potential with subsequent alteration of mitochondrial structure and shape^[52].

Owing to the existence of an extensive population of mitochondria inside the cardiac muscles, there will be a plenty of mitochondria that generate free radicals^[22]. Chaiswing *et al.*,^[49] reported that the mitochondria were the primary site for injury caused by DOX followed by secondary affection of other cellular structures. Interestingly, in the same study they have reported that mitochondrial injury coincides with the formation of aldehyde adducts within mitochondrial proteins, which emphasis on the role played by these toxic aldehyde in the pathogenesis of DOX induced mitochondrial injury. As a consequence of mitochondrial injury, oxidative phosphorylation decreases and muscles shift to anaerobic metabolism with formation of lactic acid with a subsequent increase in intracellular acidity. Such acidity can further alter the activity of the enzymes responsible for fundamental components production like proteins and phospholipids, causing more damage to the cellular components^[53].

Histological sections of DOX+Alda group showed evident protection exerted by Alda-1 on the cardiac muscle fibers with remarkable preservation of their structure. These findings were further confirmed by the electron microscope, where remarkable improvement in the ultrastructure of cardiomyocytes was evident. The cardiomyocytes markedly retained their normal appearance with regularly arranged myofibrils and preserved sarcomere continuity as well as remarkable preservation of the mitochondrial structure. Similar findings were reported after acute DOX exposure in ALDH2 overexpressing transfected C57BL6 mice^[54]. Moreover, in the same study, DOX-

induced alterations were accentuated in ALDH2 knockout mice. This supported the protective effect of ALDH2 on myocardial histology after DOX administration.

Histological results went hand in hand with biochemical results of biomarkers of cardiac tissue injury and oxidative stress. Concomitant administration of Alda-1 with DOX significantly decreased the elevated serum cardiac enzymes CK-MB and LDH. Also, it significantly escalated TAC in comparison to DOX group. Although, Alda-1 decreased the MDA level in the cardiac tissue and was insignificant as compared to the control, this reduction was still statistically insignificant from DOX treated group, this could be explained by MDA measurement during peak time of the lipid peroxidation. Where, Kang *et al.*,^[55] have reported that, after 20mg/kg of doxorubicin, lipid peroxidation reaches its maximum level after the same duration of measuring as the current study.

Ge *et al.*,^[56] have suggested that ALDH2 protection toward DOX-triggered cardiac injury was offered via the maintenance of mitochondrial integrity. They declared that ALDH2 was able to rescue the mitochondria from DOX-induced dysfunction of mitochondrial membrane potential, mitochondrial proteins and mitochondrial enzymes injury, in addition to attenuation of DOX-induced elevation of 4HNE toxic aldehyde levels.

From the above-mentioned facts, it is postulated that protection of the mitochondrial ultrastructure observed in Alda+DOX group could play a role in the overall preservation of the tissue architecture and organ weight. Furthermore, mitochondrial morphometry was done in the current study to assess mitochondrial size changes after DOX exposure. Results displayed a significantly larger mitochondrial size in DOX group in contrast with all other studied groups indicating mitochondrial swelling. This went in line with Khiati *et al.*,^[57] who reported swelling of the mitochondria after its morphometric surface area analysis in DOX-induced myocardial intoxication. On the other hand, concomitant administration of Alda-1 with DOX has further confirmed the preservation of the mitochondrial structure where mitochondrial size in DOX +Alda-1 group has displayed no significant difference versus the control and Alda groups.

It is well established that DOX causes disturbance in the calcium homeostasis. Lipid peroxidation of the cellular membranes induced by DOX can lead to alteration of their residing proteins. DOX impairs sarcoplasmic reticulum Ca²⁺-ATPase 2 (SERCA2) on the sarcoplasmic tubule membranes, whose function is to maintain basal intracellular calcium level by promoting calcium reuptake into the sarcoplasmic tubules. DOX alteration to SERCA2 leads to intracellular calcium overload^[58]. This could explain the shortening of the sarcomeres observed in the current work which could be attributed to sustained contraction of cardiac muscle fibers^[59]. In the current work, Alda-1 has preserved normal striation pattern of the sarcomeres and the structure of the sarcotubular system as

observed by TEM in DOX +Alda-1 group. Other studies have reported that ALDH2 was able to restore impaired calcium regulation after DOX administration, where it mitigated the elevation of intracellular calcium levels as well as the downregulation of SERCA2 induced by DOX, thus rescuing against cardiomyocyte contractile dysfunction^[54,56].

Previous researches^[48,60-62] proved that DOX-triggered oxidative stress stimulates apoptosis in addition to necrosis. Apoptosis is either induced by DOX concentration inside the mitochondria that mediates cytochrome C liberation, or through calcium overload generation that will in turn also mediates cytochrome C liberation and induces apoptosis by activated caspases^[63]. This could account for the focal loss of fibers and decreased heart weight observed in DOX group. Moreover, the wavy fibers observed following administration of DOX could result from the systolic tugs formed by the viable contractile fibers nearby to the non-contractile one, thus stretching them^[64]. In addition, the hyperoesinophilic fibers observed in DOX group could be explained by the intensified attachment of eosin to the denatured proteins of the cardiac muscle fibers. Overtime, these dead cells will develop paler cytoplasm^[65]. Furthermore, in the current work, nuclear alterations were observed in DOX group such as the darkly stained nuclei observed by light microscope as well as the irregular nuclei with peripheral condensation of chromatin seen by electron microscope. Similar nuclear changes were observed in other studies after DOX administration^[40,66,67]. They reported that these nuclear changes can be attributed to dox induced apoptosis and DOX further intercalation inside the nuclear DNA with its consequent deformation^[66,67]. Where, Asam *et al.*,^[67] showed localization of doxorubicin intracellularly inside the nucleus by fluorescence microscope. Dox interaction with the DNA and its intercalation deforms the DNA, thus hinder its replication, thus it is particularly toxic to rapidly dividing cells as well as cancer cells. Moreover, Lu *et al.*,^[66] also reported nuclear condensation in association with apoptosis and decreased cells viability *in-vitro* following doxorubicin treatment.

It has been reported that activated ALDH2 using Alda-1 has antagonized DOX-triggered apoptosis via reduction of the oxidative stress and the accumulated aldehydes which in turn is reflected on improvement of the myocardial structure and the biochemical markers^[14]. In addition to Alda-1 anti-apoptotic effect, it possesses an anti-inflammatory effect which lessens different pathologies inducing inflammation and cellular infiltration. Thus Alda-1 was reported to lessen apoptosis, necrosis as well as inflammation and guard against mitochondrial injury^[16,68-71]. Another proposed mechanism for ALDH2 amelioration of DOX-triggered myocardial damage is thought to be, through regulation of autophagy^[54]. Autophagy is a mechanism where defective organelles and other cellular components are degraded and recycled through lysosomal digestion in order to keep only the functional one. Although beneficial, excessive autophagy can cause cell death^[12,54,72]. Interestingly,

decreased ALDH2 and increased autophagy was also observed in left ventricular myocardium of patient with idiopathic dilated cardiomyopathy, suggesting a possible correlation between ALDH2 and cardiomyopathy^[54]. In the current study, lysosomes were more frequently observed by TEM in DOX group. In addition, autophagosome formation was also detected in the same group. Similar findings were documented using TEM in other studies after DOX administration^[73,74]. They suggested that these findings indicates the initiation of the process of autophagy, where during autophagy, organelles and proteins are trapped inside a double membrane vesicle called autophagosome before being digested by lysosomes. Koleini and Kardami,^[75] have suggested that incompleteness of autophagy occurring via DOX-induced lysosomal dysfunction leads to accumulation of undegraded structures that promotes increased ROS production and eventually cell death.

In the present work, collagen fibers were infrequently encountered in the interstitial spaces of DOX-treated group by using the electron microscope. However, no significant increase in collagen deposition was encountered in trichrome-stained sections between all studied groups (data not shown). This could be explained by a short duration of exposure to DOX that needs to be elongated to induce myocardial fibrosis. Moreover, in line with our finding Mukhopadhyay *et al.*,^[76] reported that myocardial fibrosis could not be detected in acute cardiotoxicity model 5 days after 20 mg/kg DOX exposure in mice neither by staining techniques nor by biochemical fibrosis markers. In contrary, in the same study fibrosis was detectable after 35 days of DOX chronic exposure

Thus, the current work offers clear histological evidence of DOX-induced toxicity on the myocardium via oxidative stress and its subsequent lipid peroxidation. Alda-1 showed a pronounced protection in DOX-triggered cardiotoxicity as indicated by improvement in the heart weight, the structure of the myocardium and the biochemical markers. However, some residual changes were still depicted.

CONCLUSION

ALDH2 targeting is a promising new modality offering protective potentials against DOX-induced cardiac toxicity. Yet, more studies are needed to afford it for future therapeutic application.

ABBREVIATIONS

Alda-1: aldehyde dehydrogenase agonist-1, **ALDH2:** aldehyde dehydrogenase 2 enzyme, **CK-MB:** creatinine kinase- MB, **DNA:** deoxyribonucleic acid, **DOX:** doxorubicin, **H&E:** Haematoxylin and Eosin, **4HNE:** 4-hydroxy-2-nonenal, **LDH:** lactate dehydrogenase, **MDA:** malondialdehyde, **MRI:** Magnetic resonance imaging, **RBCs:** red blood corpuscles, **ROS:** reactive oxygen species, **SERCA2:** sarcoplasmic reticulum Ca²⁺-ATPase 2, **TAC:** total antioxidant capacity, **TEM:** transmission electron microscopic.

CONFLICT OF INTERESTS

There are no conflicts of interest.

REFERENCES

- Wallace KB, Sardão VA, Oliveira PJ. Mitochondrial Determinants of Doxorubicin-Induced Cardiomyopathy. *Circulation research*. 2020;126(7):926-41.
- Bulten BF, Sollini M, Boni R, Massri K, de Geus-Oei L-F, van Laarhoven HW, *et al.* Cardiac molecular pathways influenced by doxorubicin treatment in mice. *Scientific reports*. 2019;9(1):1-10.
- Wang S, Wang Y, Zhang Z, Liu Q, Gu J. Cardioprotective effects of fibroblast growth factor 21 against doxorubicin-induced toxicity via the SIRT1/LKB1/AMPK pathway. *Cell Death Dis*. 2017;8(8):e3018.
- Renu K, V GA, P BT, Arunachalam S. Molecular mechanism of doxorubicin-induced cardiomyopathy - An update. *Eur J Pharmacol*. 2018;818:241-53.
- Kim SH, Kim KJ, Kim JH, Kwak JH, Song H, Cho JY, *et al.* Comparison of doxorubicin-induced cardiotoxicity in the ICR mice of different sources. *Lab Anim Res*. 2017;33(2):165-70.
- Rodríguez-Lara SQ, Cardona-Muñoz EG, Ramírez-Lizardo EJ, Totsuka-Sutto SE, Castillo-Romero A, García-Cobián TA, *et al.* Alternative Interventions to Prevent Oxidative Damage following Ischemia/Reperfusion. *Oxidative medicine and cellular longevity*. 2016;2016:7190943-.
- Chen CH, Ferreira JC, Gross ER, Mochly-Rosen D. Targeting aldehyde dehydrogenase 2: new therapeutic opportunities. *Physiol Rev*. 2014;94(1):1-34.
- Xu H, Zhang Y, Ren J. ALDH2 and Stroke: A Systematic Review of the Evidence. In: Ren J, Zhang Y, Ge J, editors. *Aldehyde Dehydrogenases: From Alcohol Metabolism to Human Health and Precision Medicine*. Singapore: Springer Singapore; 2019. p. 195-210.
- Raub AG, Hwang S, Horikoshi N, Cunningham AD, Rahighi S, Wakatsuki S, *et al.* Small-Molecule Activators of Glucose-6-phosphate Dehydrogenase (G6PD) Bridging the Dimer Interface. *ChemMedChem*. 2019;14(14):1321-4.
- Gomes KM, Campos JC, Bechara LR, Queliconi B, Lima VM, Disatnik MH, *et al.* Aldehyde dehydrogenase 2 activation in heart failure restores mitochondrial function and improves ventricular function and remodelling. *Cardiovasc Res*. 2014;103(4):498-508.
- Gomes KMS, Bechara LRG, Lima VM, Ribeiro MAC, Campos JC, Dourado PM, *et al.* Aldehydic load and aldehyde dehydrogenase 2 profile during the progression of post-myocardial infarction cardiomyopathy: Benefits of Alda-1. *International Journal of Cardiology*. 2015;179:129-38.

12. Ji W, Wei S, Hao P, Xing J, Yuan Q, Wang J, *et al.* Aldehyde Dehydrogenase 2 Has Cardioprotective Effects on Myocardial Ischaemia/Reperfusion Injury via Suppressing Mitophagy. *Front Pharmacol.* 2016;7:101.
13. Hu Y, Yan JB, Zheng MZ, Song XH, Wang LL, Shen YL, *et al.* Mitochondrial aldehyde dehydrogenase activity protects against lipopolysaccharide-induced cardiac dysfunction in rats. *Molecular medicine reports.* 2015;11(2):1509-15.
14. Gao Y, Xu Y, Hua S, Zhou S, Wang K. ALDH2 attenuates Dox-induced cardiotoxicity by inhibiting cardiac apoptosis and oxidative stress. *International journal of clinical and experimental medicine.* 2015;8(5):6794.
15. Wang L, Zhang T-P, Zhang Y, Bi H-L, Guan X-M, Wang H-X, *et al.* Protection against doxorubicin-induced myocardial dysfunction in mice by cardiac-specific expression of carboxyl terminus of hsp70-interacting protein. *Scientific reports.* 2016;6(1):1-14.
16. Zhu Q, He G, Wang J, Wang Y, Chen W. Pretreatment with the ALDH2 agonist Alda-1 reduces intestinal injury induced by ischaemia and reperfusion in mice. *Clinical science.* 2017;131(11):1123-36.
17. Bancroft JD, Layton C. The hematoxylin and eosin. *Bancroft's theory and practice of histological techniques.* 2012:173-86.
18. Kuo J. *Electron microscopy: methods and protocols:* Springer Science & Business Media; 2007.
19. Bishop JB, Tani Y, Witt K, Johnson JA, Peddada S, Dunnick J, *et al.* Mitochondrial Damage Revealed by Morphometric and Semiquantitative Analysis of Mouse Pup Cardiomyocytes Following in Utero and Postnatal Exposure to Zidovudine and Lamivudine. *Toxicological Sciences.* 2004;81(2):512-7.
20. Kirkpatrick L, Feeney B. *A Simple Guide to IBM SPSS Statistics for version 20.0.* Student ed. Belmont, Calif: wadsworth, Cengage Learning; 2013.
21. Sheibani M, Nezamoleslami S, Faghir-Ghanesefat H, Emami Ah, Dehpour AR. Cardioprotective effects of dapson against doxorubicin-induced cardiotoxicity in rats. *Cancer Chemotherapy and Pharmacology.* 2020;85(3):563-71.
22. Hu X, Li B, Li L, Li B, Luo J, Shen B. Asiatic Acid Protects against Doxorubicin-Induced Cardiotoxicity in Mice. *Oxidative Medicine and Cellular Longevity.* 2020;2020:5347204.
23. Štěrba M, Popelová O, Vávrová A, Jirkovský E, Kovaříková P, Geršl V, *et al.* Oxidative stress, redox signaling, and metal chelation in anthracycline cardiotoxicity and pharmacological cardioprotection. *Antioxidants & redox signaling.* 2013;18(8):899-929.
24. Forman HJ, Davies KJ, Ursini F. How do nutritional antioxidants really work: nucleophilic tone and para-hormesis versus free radical scavenging in *in vivo*. *Free Radical Biology and Medicine.* 2014;66:24-35.
25. Chen C-H, Budas GR, Churchill EN, Disatnik M-H, Hurley TD, Mochly-Rosen D. Activation of aldehyde dehydrogenase-2 reduces ischemic damage to the heart. *Science.* 2008;321(5895):1493-5.
26. Perez-Miller S, Younus H, Vanam R, Chen C-H, Mochly-Rosen D, Hurley TD. Alda-1 is an agonist and chemical chaperone for the common human aldehyde dehydrogenase 2 variant. *Nature structural & molecular biology.* 2010;17(2):159.
27. Li C, Sun W, Gu C, Yang Z, Quan N, Yang J, *et al.* Targeting ALDH2 for therapeutic interventions in chronic pain-related myocardial ischemic susceptibility. *Theranostics.* 2018;8(4):1027.
28. Gong D, Zhang Y, Zhang H, Gu H, Jiang Q, Hu S. Aldehyde dehydrogenase-2 activation during cardioplegic arrest enhances the cardioprotection against myocardial ischemia-reperfusion injury. *Cardiovasc Toxicol.* 2012;12(4):350-8.
29. Fu SH, Zhang HF, Yang ZB, Li TB, Liu B, Lou Z, *et al.* Alda-1 reduces cerebral ischemia/reperfusion injury in rat through clearance of reactive aldehydes. *Naunyn Schmiedeberg Arch Pharmacol.* 2014;387(1):87-94.
30. Garcia-Menendez L, Karamanlidis G, Kolwicz S, Tian R. Substrain specific response to cardiac pressure overload in C57BL/6 mice. *Am J Physiol Heart Circ Physiol.* 2013;305(3):H397-402.
31. Grant MKO, Seelig DM, Sharkey LC, Zordoky BN. Sex-dependent alteration of cardiac cytochrome P450 gene expression by doxorubicin in C57Bl/6 mice. *Biology of sex differences.* 2017;8:1-.
32. Willis MS, Parry TL, Brown DI, Mota RI, Huang W, Beak JY, *et al.* Doxorubicin Exposure Causes Subacute Cardiac Atrophy Dependent on the Striated Muscle-Specific Ubiquitin Ligase MuRF1. *Circ Heart Fail.* 2019;12(3):e005234.
33. Tedesco L, Rossi F, Ragni M, Ruocco C, Brunetti D, Carruba MO, *et al.* A Special Amino-Acid Formula Tailored to Boosting Cell Respiration Prevents Mitochondrial Dysfunction and Oxidative Stress Caused by Doxorubicin in Mouse Cardiomyocytes. *Nutrients.* 2020;12(2):282.
34. Shaker RA, Abboud SH, Assad HC, Hadi N. Enoxaparin attenuates doxorubicin induced cardiotoxicity in rats via interfering with oxidative stress, inflammation and apoptosis. *BMC Pharmacology and Toxicology.* 2018;19(1):1-10.
35. Octavia Y, Kararigas G, de Boer M, Chrifi I, Kietadisorn R, Swinnen M, *et al.* Folic acid reduces doxorubicin-induced cardiomyopathy by modulating endothelial nitric oxide synthase. *J Cell Mol Med.* 2017;21(12):3277-87.

36. Li K, Sung RYT, Huang WZ, Yang M, Pong NH, Lee SM, *et al.* Thrombopoietin Protects Against In *Vitro* and In *Vivo* Cardiotoxicity Induced by Doxorubicin. *Circulation*. 2006;113(18):2211-20.
37. Bin Jordan YA, Ansari MA, Raish M, Alkharfy KM, Ahad A, Al-Jenoobi FI, *et al.* Sinapic Acid Ameliorates Oxidative Stress, Inflammation, and Apoptosis in Acute Doxorubicin-Induced Cardiotoxicity via the NF- κ B-Mediated Pathway. *BioMed Research International*. 2020;2020:3921796.
38. Aziz MM, Abd El Fattah MA, Ahmed KA, Sayed HM. Protective effects of olmesartan and l-carnitine on doxorubicin-induced cardiotoxicity in rats. *Can J Physiol Pharmacol*. 2020;98(4):183-93.
39. Li W-J, Zhang X-Y, Wu R-T, Song Y-H, Xie M-Y. Ganoderma atrum polysaccharide improves doxorubicin-induced cardiotoxicity in mice by regulation of apoptotic pathway in mitochondria. *Carbohydrate Polymers*. 2018;202:581-90.
40. Sergazy S, Shulgau Z, Fedotovskikh G, Chulenbayeva L, Nurgozhina A, Nurgaziyev M, *et al.* Cardioprotective effect of grape polyphenol extract against doxorubicin induced cardiotoxicity. *Scientific Reports*. 2020;10(1):14720.
41. Al-Harathi SE, Alarabi OM, Ramadan WS, Alaama MN, Al-Kreathy HM, Damanhoury ZA, *et al.* Amelioration of doxorubicin-induced cardiotoxicity by resveratrol. *Mol Med Rep*. 2014;10(3):1455-60.
42. Krishnamurthy B, Rani N, Bharti S, Golechha M, Bhatia J, Nag TC, *et al.* Febuxostat ameliorates doxorubicin-induced cardiotoxicity in rats. *Chem Biol Interact*. 2015;237:96-103.
43. Koracevic D, Koracevic G, Djordjevic V, Andrejevic S, Cosic V. Method for the measurement of antioxidant activity in human fluids. *Journal of clinical pathology*. 2001;54(5):356-61.
44. Sotoudeh Anvari M, Mortazavian Babaki M, Boroumand MA, Eslami B, Jalali A, Goodarzynejad H. Relationship between calculated total antioxidant status and atherosclerotic coronary artery disease. *Anatolian journal of cardiology*. 2016;16(9):689-95.
45. Soni H, Pandya G, Patel P, Acharya A, Jain M, Mehta AA. Beneficial effects of carbon monoxide-releasing molecule-2 (CORM-2) on acute doxorubicin cardiotoxicity in mice: role of oxidative stress and apoptosis. *Toxicol Appl Pharmacol*. 2011;253(1):70-80.
46. Zhang Y, Kang Y-M, Tian C, Zeng Y, Jia L-X, Ma X, *et al.* Overexpression of Nrdp1 in the Heart Exacerbates Doxorubicin-Induced Cardiac Dysfunction in Mice. *PLOS ONE*. 2011;6(6):e21104.
47. Jungsuwadee P. Doxorubicin-induced cardiomyopathy: an update beyond oxidative stress and myocardial cell death. *Cardiovascular Regenerative Medicine*. 2016;3.
48. Cappetta D, De Angelis A, Sapio L, Prezioso L, Illiano M, Quaini F, *et al.* Oxidative Stress and Cellular Response to Doxorubicin: A Common Factor in the Complex Milieu of Anthracycline Cardiotoxicity. *Oxid Med Cell Longev*. 2017;2017:1521020.
49. Chaiswing L, Cole MP, St. Clair DK, Ittarat W, Szweda LI, Oberley TD. Oxidative Damage Precedes Nitrate Damage in Adriamycin-Induced Cardiac Mitochondrial Injury. *Toxicologic Pathology*. 2004;32(5):536-47.
50. Aryal B, Rao VA. Deficiency in Cardiolipin Reduces Doxorubicin-Induced Oxidative Stress and Mitochondrial Damage in Human B-Lymphocytes. *PLOS ONE*. 2016;11(7):e0158376.
51. Ayala A, Muñoz MF, Argüelles S. Lipid Peroxidation: Production, Metabolism, and Signaling Mechanisms of Malondialdehyde and 4-Hydroxy-2-Nonenal. *Oxidative Medicine and Cellular Longevity*. 2014;2014:360438.
52. Chen L, Lang AL, Poff GD, Ding W-X, Beier JI. Vinyl chloride-induced interaction of nonalcoholic and toxicant-associated steatohepatitis: Protection by the ALDH2 activator Alda-1. *Redox Biology*. 2019;24:101205.
53. Borović ML, Ičević I, Kanački Z, Žikić D, Seke M, Injac R, *et al.* Effects of fullereneol C60(OH)24 nanoparticles on a single-dose doxorubicin-induced cardiotoxicity in pigs: an ultrastructural study. *Ultrastruct Pathol*. 2014;38(2):150-63.
54. Sun A, Cheng Y, Zhang Y, Zhang Q, Wang S, Tian S, *et al.* Aldehyde dehydrogenase 2 ameliorates doxorubicin-induced myocardial dysfunction through detoxification of 4-HNE and suppression of autophagy. *J Mol Cell Cardiol*. 2014;71:92-104.
55. Kang YJ, Chen Y, Epstein PN. Suppression of doxorubicin cardiotoxicity by overexpression of catalase in the heart of transgenic mice. *J Biol Chem*. 1996;271(21):12610-6.
56. Ge W, Yuan M, Ceylan AF, Wang X, Ren J. Mitochondrial aldehyde dehydrogenase protects against doxorubicin cardiotoxicity through a transient receptor potential channel vanilloid 1-mediated mechanism. *Biochimica et Biophysica Acta (BBA) - Molecular Basis of Disease*. 2016;1862(4):622-34.
57. Khiati S, Dalla Rosa I, Sourbier C, Ma X, Rao VA, Neckers LM, *et al.* Mitochondrial topoisomerase I (top1mt) is a novel limiting factor of doxorubicin cardiotoxicity. *Clin Cancer Res*. 2014;20(18):4873-81.

58. Murabito A, Hirsch E, Ghigo A. Mechanisms of Anthracycline-Induced Cardiotoxicity: Is Mitochondrial Dysfunction the Answer? *Frontiers in cardiovascular medicine*. 2020;7:35-.
59. Omar AM, Meleis AE, Arfa SA, Zahran NM, Mehanna RA. Comparative Study of the Therapeutic Potential of Mesenchymal Stem Cells Derived from Adipose Tissue and Bone Marrow on Acute Myocardial Infarction Model. *Oman Med J*. 2019;34(6):534-43.
60. Arola OJ, Saraste A, Pulkki K, Kallajoki M, Parvinen M, Voipio-Pulkki L-M. Acute doxorubicin cardiotoxicity involves cardiomyocyte apoptosis. *Cancer research*. 2000;60(7):1789-92.
61. Ekinci Akdemir FN, Yildirim S, Kandemir FM, Tanyeli A, Küçükler S, Bahaeddin Dortbudak M. Protective effects of gallic acid on doxorubicin-induced cardiotoxicity; an experimental study. *Archives of Physiology and Biochemistry*. 2019:1-8.
62. Razmaraii N, Babaei H, Mohajjel Nayebi A, Assadnassab G, Ashrafi Helan J, Azarmi Y. Crocin treatment prevents doxorubicin-induced cardiotoxicity in rats. *Life Sci*. 2016;157:145-51.
63. Mitry MA, Edwards JG. Doxorubicin induced heart failure: Phenotype and molecular mechanisms. *IJC heart & vasculature*. 2016;10:17-24.
64. Kumar V, Abbas AK, Fausto N, Aster JC. Robbins and Cotran pathologic basis of disease, professional edition e-book: Elsevier health sciences; 2014.
65. Miller MA, Zachary JF. Mechanisms and Morphology of Cellular Injury, Adaptation, and Death. *Pathologic Basis of Veterinary Disease*. 2017:2-43.e19.
66. Lu J, Li J, Hu Y, Guo Z, Sun D, Wang P, *et al*. Chrysophanol protects against doxorubicin-induced cardiotoxicity by suppressing cellular PARYlation. *Acta Pharmaceutica Sinica B*. 2019;9(4):782-93.
67. Asam C, Buerger K, Felthaus O, Brébant V, Rachel R, Prantl L, *et al*. Subcellular localization of the chemotherapeutic agent doxorubicin in renal epithelial cells and in tumor cells using correlative light and electron microscopy. *Clin Hemorheol Microcirc*. 2019;73(1):157-67.
68. Li M, Xu M, Li J, Chen L, Xu D, Tong Y, *et al*. Alda-1 Ameliorates Liver Ischemia-Reperfusion Injury by Activating Aldehyde Dehydrogenase 2 and Enhancing Autophagy in Mice. *Journal of Immunology Research*. 2018;2018:9807139.
69. Liu Z, Ye S, Zhong X, Wang W, Lai CH, Yang W, *et al*. Pretreatment with the ALDH2 activator Alda-1 protects rat livers from ischemia/reperfusion injury by inducing autophagy. *Molecular Medicine Reports*. 2020;22(3):2373-85.
70. Cao S, Bian Y, Zhou X, Yuan Q, Wei S, Xue L, *et al*. A small-molecule activator of mitochondrial aldehyde dehydrogenase 2 reduces the severity of cerulein-induced acute pancreatitis. *Biochemical and Biophysical Research Communications*. 2020;522(2):518-24.
71. Ding J, Zhang Q, Luo Q, Ying Y, Liu Y, Li Y, *et al*. Alda-1 Attenuates Lung Ischemia-Reperfusion Injury by Reducing 4-Hydroxy-2-Nonenal in Alveolar Epithelial Cells. *Crit Care Med*. 2016;44(7):e544-52.
72. Guo B, Tam A, Santi SA, Parissenti AM. Role of autophagy and lysosomal drug sequestration in acquired resistance to doxorubicin in MCF-7 cells. *BMC Cancer*. 2016;16(1):762.
73. Kawaguchi T, Takemura G, Kanamori H, Takeyama T, Watanabe T, Morishita K, *et al*. Prior starvation mitigates acute doxorubicin cardiotoxicity through restoration of autophagy in affected cardiomyocytes. *Cardiovascular Research*. 2012;96(3):456-65.
74. Dhingra R, Margulets V, Chowdhury SR, Thliveris J, Jassal D, Fernyhough P, *et al*. Bnip3 mediates doxorubicin-induced cardiac myocyte necrosis and mortality through changes in mitochondrial signaling. *Proc Natl Acad Sci U S A*. 2014;111(51):E5537-44.
75. Koleini N, Kardami E. Autophagy and mitophagy in the context of doxorubicin-induced cardiotoxicity. *Oncotarget*. 2017;8(28):46663-80.
76. Mukhopadhyay P, Rajesh M, Bátkai S, Patel V, Kashiwaya Y, Liaudet L, *et al*. CB1 cannabinoid receptors promote oxidative stress and cell death in murine models of doxorubicin-induced cardiomyopathy and in human cardiomyocytes. *Cardiovascular research*. 2010;85(4):773-84.

المخلص العربي

التأثير الوقائي المحتمل للمادة المنشطة لانزيم الالدهيد المختزل ٢ (Alda-١) على السمية المحدثة بدكسوروبيسين على خلايا عضلة البطين الايسر لذكور الفئران البالغة

ايمان محمد نبيل^١، وفاء عبد الرحمن أحمد^٢، سلوي سعيد السبع^٣، رانا احمد ابو الروس^٤،
نانسي محمد السقيلي^٢

^١قسم علم الأنسجة وبيولوجيا الخلايا، ^٢قسم التشريح الادمي وعلم الأجنة، كلية الطب، جامعه الإسكندرية

المقدمة: دوكسوروبيسين هو دواء فعال يستخدم كمضاد للأورام. ولكن يمثل ما يسببه هذا الدواء من سمية على القلب عقبة رئيسية تحد من استخدامه. ولذلك، فهناك حاجة ماسة إلى استخدام عامل وقائي جديد للحماية من هذه الآثار. لقد اكتسبت مؤخرًا عملية تنشيط الإنزيمات اهتمامًا كبيرًا كإستراتيجية علاجية جديدة. ومن هذا المنطلق، فلقد برزت حديثًا مادة الAlda-١ في مجال حماية القلب وذلك من خلال تنشيط إنزيم الالدهيد المختزل ٢.

الهدف من البحث: تقييم التأثير الوقائي المحتمل للمادة المنشطة لانزيم الالدهيد المختزل ٢ (مادة Alda-١) على السمية التي يسببها دوكسوروبيسين على القلب.

مواد وطرق البحث: تم تقسيم ٢٤ من ذكور الفئران البالغة إلى ٤ مجموعات متساوية. تلقت المجموعة الأولى الضابطة محلول ملحي عن طريق الحقن داخل الغشاء البريتوني. بينما تلقت المجموعة الثانية Alda-١ بجرعة ١٠ مجم/كجم من وزن الجسم عن طريق الحقن داخل الغشاء البريتوني يوميًا لمدة ٥ أيام. وتلقت المجموعة الثالثة حقنة واحدة داخل الغشاء البريتوني للبطن من الدوكسوروبيسين بجرعة ٢٠ مجم/كجم من وزن الجسم. بينما تلقت المجموعة الرابعة كلاً من الدوكسوروبيسين و Alda-١ معاً كما هو الحال في المجموعتين الثانية والثالثة، وبدأ حقن Alda-١ يوم واحد قبل دوكسوروبيسين. وقد تمت التضحية بجميع الفئران في اليوم الخامس من إعطاء الدوكسوروبيسين، وجمعت عينات الدم، كما تم تشريح القلوب وتحضير العينات للدراسة التشريحية وكذلك النسيجية والبيو كيميائية.

النتائج: لقد تسبب دواء دوكسوروبيسين في احداث سمية شديدة على القلب، كما هو واضح من الانخفاض الملحوظ في وزن القلب وكذلك من الاعتلال الشديد الذي أظهره الفحص المجهرى الضوئي والإلكتروني في نسيج عضلة القلب. علاوة على ذلك، فلقد ادى الي ارتفاع مستويات المؤشرات الحيوية لإصابة عضلة القلب (CK-MB & LDH) في الدم بشكل ملحوظ. كما تسبب دوكسوروبيسين في زيادة الأكسدة وذلك عن طريق الانخفاض الكبير في إجمالي القدرة المضادة للأكسدة في مصل الفئران والزيادة في مستويات مالونديالدهيد في الأنسجة. كما أظهرت الدراسة القياسية لحجم الميتوكوندريا زيادتها في الحجم. في المقابل، فإن إعطاء Alda-١ مصاحباً لدوكسوروبيسين قد خفف من إصابة القلب بشكل ملحوظ، حيث ادى الي استعادة وزن القلب وحماية نسيج القلب جنباً إلى جنب مع الحفاظ على بنية الميتوكوندريا. علاوة على ذلك، فقد انخفضت مستويات المؤشرات الحيوية لإصابة عضلة القلب ومؤشرات زيادة الأكسدة.

الاستنتاج: يمتلك Alda-١ تأثيراً وقائياً فعالاً ضد سمية القلب الناتجة عن تعاطي دوكسوروبيسين.